Experimental Study of Thermal Management and Enhancement of Adsorption-Based Onboard Hydrogen Storage System

Hailei Wang
Department of Mechanical and Aerospace Engineering,
Utah State University,
Logan, UT 84322
e-mail: hailei.wang@usu.edu

Daniel C. Miller
Department of Mechanical Engineering,
Colorado School of Mines,
Golden, CO 80401
e-mail: dawuda@gmail.com

Although hydrogen has one of the highest specific energies, its energy density in terms of volume is very poor compared to liquid fuels. Thus, to achieve attractive energy density for hydrogen, either high-pressure compression or a storage method is needed. For onboard (vehicles) hydrogen storage, up to 700 bars are needed for commercial fuel cell vehicles. This creates extreme requirements for material strength and thus safety concerns. A new metal-organic framework 5 (MOF-5) was selected as the adsorbent for H_2 storage, as it provides promising storage capacity and is commercially available. Under the same H_2 storage capacity and tank volume, the adsorption system is expected several folds reduction in pressure. Under the current study, a unique thermal management design using Modular Adsorbing Tank Insert (MATI) is paired with conduction-enhanced compressed MOF-5 beds. Compared to bare beds without conduction enhancement, all beds with conduction enhancement using either aluminum pins or expanded natural graphite (ENG) have shown various levels of improvement on bed thermal response, which can potentially help expedite system charge and discharge cycle times for real applications.
[DOI: 10.1115/1.4050508]

Keywords: thermal management, hydrogen storage, metal-organic famework, MOF-5, conduction enhancement

Introduction

As an enabling technology for fuel cell vehicles, hydrogen storage plays a critical role in determining vehicle drive range [1–3]. As part of the Hydrogen Storage Engineering Center of Excellence (HSECoE) effort, several material-based storage concepts at cryogenic condition shave been proposed in order to meet Department of Energy (DOE) 2017 goals with the key storage parameters being gravimetric and volumetric capacities, charging and discharging rates [4,5]. Since the adsorption and desorption processes involve coupled heat and mass transfers—the heat is generated during adsorption while heat is needed during desorption—a sorbent thermal management system becomes critical for the overall hydrogen storage system performance. Currently, the leading candidate is what is called a flow-through system [6,7]. Instead of using a specially designed thermal management system, an excess amount of cryogenic hydrogen flows through the storage medium allowing a portion of hydrogen gas to be adsorbed while the rest of it providing the needed cooling. Although this can reduce the complexity of vehicle onboard hydrogen storage system, it adds significant burden and parasitic losses to hydrogen-filling stations.

This project uses advanced heat and mass transfer enhancement techniques, in order to gain rapid heat and mass transfer and the associated benefits for gravimetric and volumetric capacities. Essentially microscale features and phenomena with a characteristic length scale of 100–500 μm are used, taking advantage of their short diffusion lengths. For onboard hydrogen storage system, this can significantly improve the hydrogen charging rate, as well as the discharge rate in response to changing drive conditions. This application led to the development of a Modular Adsorbing Tank Insert (MATI) concept for cryogenic adsorption hydrogen storage. The key feature of the MATI concept is to use micro-channel cooling plates and a separate cooling fluid (e.g., liquid nitrogen or LN_2) to rapidly remove both sensible and adsorption heat during charging. In addition, the design allows the use of onboard fuel cell waste heat for the discharging process, which can significantly improve the onboard efficiency of the adsorption hydrogen storage system.

MATI Design

The MATI prototype used for the current conduction enhancement study is shown in Fig. 1. In this design, the tank is filled with densified adsorption media in the form of 1.5-cm-thick beds (pucks) which have a diameter slightly less than the internal

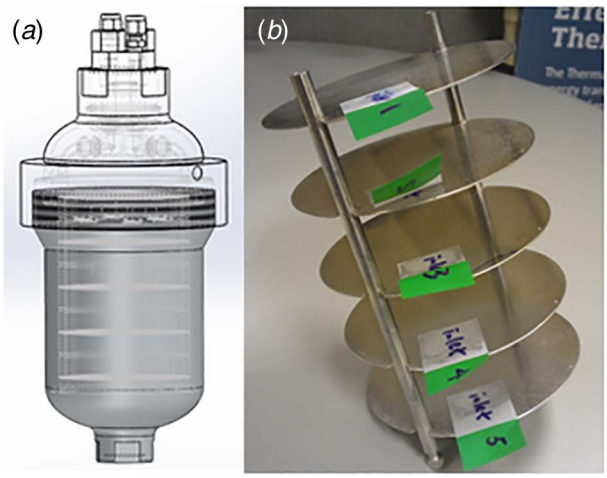

Fig. 1 (*a*) MATI prototype assembly inside of a 2-L aluminum tank and (*b*) assembled MATI cooling plate stack

Manuscript received May 15, 2020; final manuscript received March 7, 2021; published online April 2, 2021. Assoc. Editor: George Nelson.

diameter of the tank. A standard unit cell consists of a stack of a cooling plate, a media puck, a hydrogen distribution plate, a second media puck, and then a second cooling plate. During charging, hydrogen is introduced into the hydrogen distribution plate which is sandwiched between two pucks and diffuses through the puck. As the hydrogen diffuses, it is adsorbed by the media, producing heat that must be removed in order to carry on further adsorption. Simultaneously, liquid nitrogen is introduced to pass through the cooling plates. As the heat of adsorption is produced, it is conducted through the media to a cooling plate, where it is transferred to the liquid nitrogen which leaves the cooling plate at a slightly elevated temperature (90 K). The heat of adsorption is removed by two processes. First, the low-temperature hydrogen being used for adsorption is at a temperature lower than the bed temperature and will remove some of the heat of adsorption as the hydrogen increases in temperature to the temperature of the bed. The balance of the heat of adsorption is removed by having the heat conduct through the media to the liquid nitrogen through the cooling plates.

The completed MATI consists of a number of cells (typically between 10 and 50) which are connected by headers to provide liquid nitrogen to the cooling plates and collect it so that it can be exhausted from the system. In our current design, the MATI has a diameter slightly smaller than the inside diameter of the tank, forming an annular region between the outside of the MATI and the inside wall of the tank. This allows hydrogen to flow in the annular region to the hydrogen distribution plates. An alternative configuration would eliminate the annular region and utilize distribution headers to deliver and collect the hydrogen. Using distribution headers allows an increase in the diameter (approximately 2 mm or larger) and an improvement in the overall volumetric and gravimetric efficiency of the MATI. A list of specific features and benefits of the MATI design are summarized as follows:

(1) Separates cooling fluid (e.g., LN2) from charging hydrogen, which significantly reduces the consumption of cryogenic hydrogen and thus parasitic losses in hydrogen charge station.
(2) Allows the use of densified media (called pucks in this study), which can greatly improve the volumetric capacity and potentially the gravimetric capacity of the sorbent-based storage systems.
(3) Allows the use of onboard fuel cell waste heat for hydrogen desorption, which can substantially reduce parasitic losses for the fuel cell system. During hydrogen discharge, the MATI can use waste heat from the vehicle's hydrogen fuel cell to provide most of the thermal energy needed to desorb the hydrogen in the sorbent tank. Compared to the flow-through system, electric heaters are needed to raise the temperature of the sorbent beds, thus adding electric loads to the fuel cell.
(4) Enhances cooling with a separate hydrogen distribution channel between two sorbent beds (or pucks), delivering the 40 K hydrogen to the puck critical surfaces for both enhanced heat and mass transfers. As a result, puck height can be significantly increased without impacting hydrogen charging and discharging rates, thus adding positive impacts on the volumetric and gravimetric capacities.
(5) Has the flexibility of adding conduction enhancement to the pucks, which can further increase the spacing between the cooling plates. Specifically, conductive aluminum pins were embedded into the pucks to enhance their effective thermal conductivity. This became the focus of this study, which is to experimentally compare the thermal responses between blank pucks and conduction-enhanced pucks.

Conduction Enhancement

Given being commercially available, metal-organic framework 5 (MOF-5) was chosen as the hydrogen storage media. It is a microporous, crystalline solid comprised of organic linkers and Zn_4O tetrahedral clusters [8,9]. The high surface area and permanent porosity of MOF-5 make it an attractive material for a variety of applications including gas storage [10–14]. Regarding gas storage, MOF-5 has been extensively studied for automotive hydrogen storage applications [15–17]. It has also been used as the benchmark materials for newer MOFs as hydrogen storage material [18–20]. This interest stems from the observation that MOF-5 can adsorb a large amount of hydrogen up to 7.1 excess wt.% at 77 K and 40 bar [21]. Given the heat of adsorption ranging from 2 to 5 kJ/mol H_2 [22], it adds significant engineering challenges. In order to achieve targeted refueling times (e.g., the 2017 U.S. Dept. of Energy Target is 3.3 min for 5 kg H_2 [23]) and maximize the amount of hydrogen stored, it is desirable to remove the heat generated during adsorption from the MOF-5 bed in order to reach the desired adsorption temperature (e.g., 77 K).

In order to improve volumetric hydrogen density, pellet densification has been adopted [24,25]. However, some measurements on low-density MOF-5 pellets found a thermal conductivity of less than 0.08 W/m-K ($T = 45$ °C) [26]. This low conductivity places significant limitations on the design of MOF-5-based storage systems, hindering fast refueling for adsorption processes that rely on rapid temperature drop. Forming composites of MOF-5 by adding expanded natural graphite (ENG) worms has shown some promise and currently is under further investigation [27], given the high thermal conductivity (~150 W/m-K [28]) of ENG. In addition, carbons are known to be good hydrogen adsorbents [29]. Thus, the addition of ENG to MOF-5 could present a potentially promising method for improving thermal conductivity while maintaining favorable hydrogen storage characteristics.

This study, however, took an additional engineering approach by physically inserting conductive metal structures into the pucks. Figure 2 shows the conduction enhancement articles made out of aluminum pins with a pin diameter of 1/16″ (1.6 mm) and spacing of 10 mm. Based on the thermal modeling work presented in the next section, the embedded pins are expected to significantly enhance the effective thermal conductivity of the pucks, providing at least a near-term solution for the poor thermal conductivity of MOF-5. The study was thus to experimentally investigate the benefits of adding aluminum pins and ENG into the MOF-5 pucks.

Thermal Modeling

A set of modeling works were conducted to predict and quantify the improved thermal response from bare pucks (no conduction enhancement) using the embedded aluminum pin structure shown earlier. Using the most recent MOF-5 material property data made available through the HSECOE, the simulation data can also be compared with the experimental data. In order to reduce the level of complexity associated with coupled heat and mass transfer during the actual adsorption process and directly compare puck thermal performance, only sensible heat of a single puck (either bare or pin) was modeled. Figure 3 shows the temperature profiles of both pucks at the end of a five-minute cooling cycle using LN_2 at

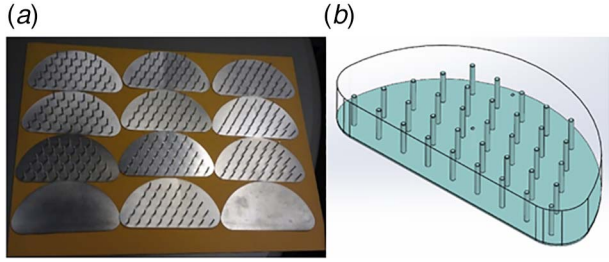

Fig. 2 (*a*) Conduction enhancement test articles with aluminum pins and (*b*) computational fluid dynamics model of conduction enhancement pins inserted into the MOF-5 pucks

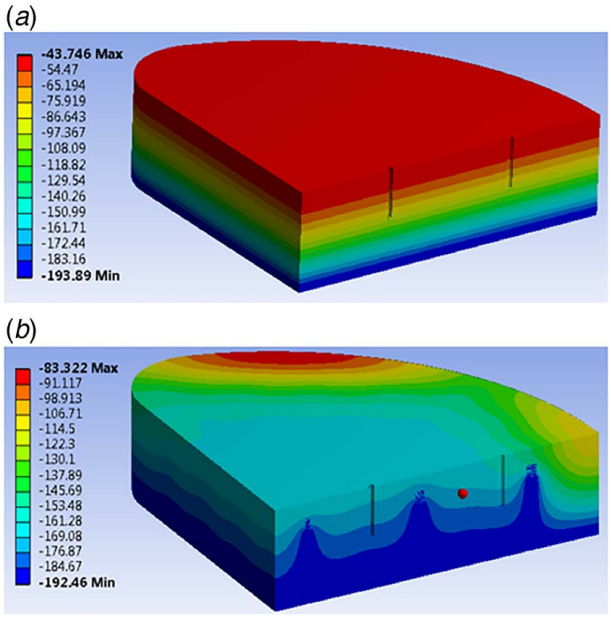

Fig. 3 Puck temperature contours (showing half puck) at end of 5-min cooling cycle: (*a*) bare puck and (*b*) pin enhanced puck

−193 °C (80 K). In both cases, the pucks were held at a room temperature of 20 °C initially. A convection boundary condition was applied to the backside of the aluminum base plate flowing LN_2 with a constant heat transfer coefficient of 1000 W/m^2-K.

The three-dimensional (3D) transient simulation was conducted using ANSYS. The mesh was refined around the aluminum pins and the two thermocouple holes with a total of 580 K elements. According to Fig. 3, the transient thermal simulation data clearly indicates the averaged puck temperature with pins is substantially cooler than that of the bare puck, which could enable the conduction-enhanced MATI design to meet the future DOE target of 3.3 min hydrogen charge time as well as volumetric and gravimetric capacities. To further compare the simulation data with later experiment results, the temperature data at one of the two thermocouple locations were plotted for both pucks shown in Fig. 4. The curve again shows the benefit of adding the conduction enhancement pins as the temperature at the thermocouple location came down significantly faster for the puck with pins.

Experimental Setup

The five cooling plates for the MATI were individually joined with headers using vacuum brazing. Orbital welding was used to connect the header tubes afterward. A picture of the assembled

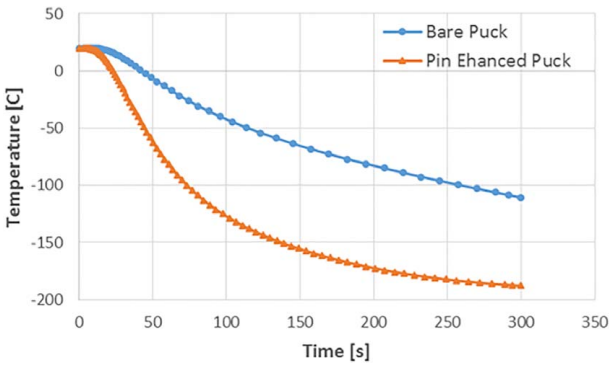

Fig. 4 Puck temperature profiles with time at one of the two thermocouple locations

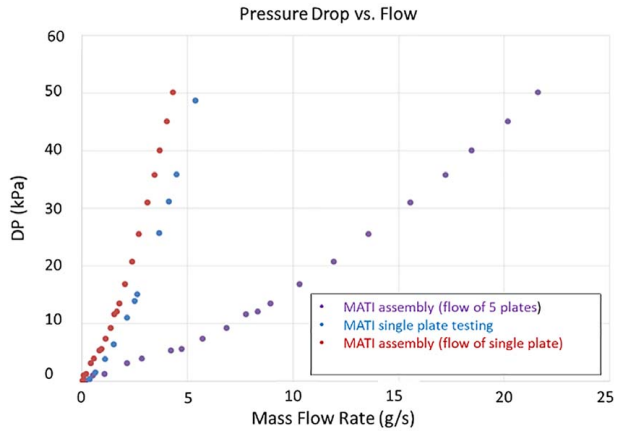

Fig. 5 Comparison of measured pressure drops as a function of flowrates (five-plate versus single plate)

MATI is shown in Fig. 1(*a*). The MATI was tested under 50 bars for over 5 min to ensure no apparent deformation and leaks were identified. Pressure drop versus flowrate was also conducted to ensure good flow. As shown in Fig. 5, the pressure drop data for the five-plate MATI assembly are compared with that of the single plate. For a given pressure drop, the assembly achieved a much higher mass flowrate (on the order of 5× of the single plate). Given the mass flowrate for the five-plate MATI, assembly is five times higher than the flow used for the single-plate test, the measured pressure drop for the MATI assembly is also plotted against the scaled flow for each of the five plates (uniform flow distribution among the plates was assumed). As shown, a slightly higher pressure drop per plate is observed based on the pressure drop measurement for the five-plate MATI assembly, which was likely due to extra pressure drops in the headers as the flowrate was five times that for the single plate.

In addition to the pressure drop testing, the MATI was tested to verify that the flow distributions in each plate were consistent prior to assembly of the MATI and MOF-5 pucks into the pressure vessel. This was done to ensure that the results of the conduction tests were not caused by a bias in the flow distributions. Testing using water at various flowrates was conducted to ensure good LN_2 flow among the cooling plates where the six pairs of pucks would be installed. Figure 6 shows the flow testing results for two different flowrates. With five cooling plates showing similar thermal response at the same location, this indicates that no flow maldistributions should be expected during the following adsorption/cooling cycle tests.

Using a combination of aluminum pins and ENG, six kinds of pucks were made for investigation—bare MOF-5, bare and random ENG (B/R), bare and layered ENG (B/L), pin and random ENG (P/R), pin and layered ENG (P/L), and pins-only MOF-5. As shown in Fig. 7, a total of 12 pucks (two of each) were assembled into the MATI. In order to monitor the puck temperatures, each puck had two thermocouple holes previously made during its forming process. One thermocouple is close to the center, and the other is away from the center, which could capture flow-related effects. Six pucks (one of each kind) were selected for instrumentation using 0.040″ sheathed T-type thermocouples as shown in Fig. 7.

While MOF-5 has shown stability in exposure to other gas impurities in a hydrogen gas environment [16], precautions were taken in preparing the experiment. Given MOF-5 is not stable in ambient air [30], assembly of the MATI and pucks was done within a positive pressure glove box to minimize exposure of the pucks to moisture from the ambient air. This helps mitigate absorption degradation during charging cycles. Due to the instrumentation configuration, thermocouples had to be fitted to the pucks prior to inserting the pucks between cooling plates. The 0.040″ thermocouples needed two sharp bends in order to be inserted into the holes in the

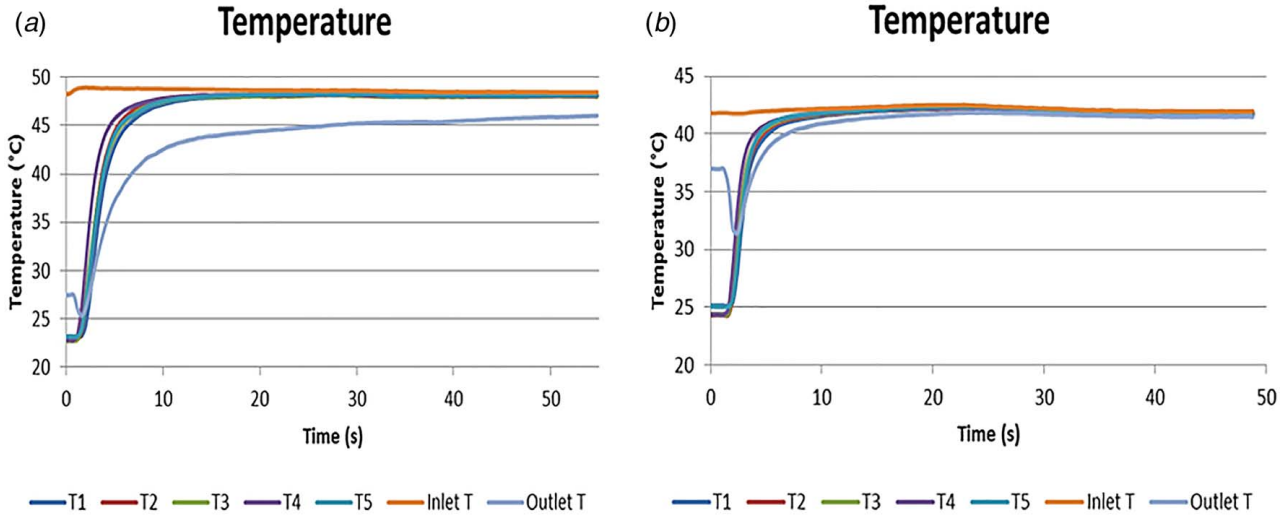

Fig. 6 Temperature response of five cooling plates T1–T5: (*a*) water flowrate = 0.73 liter per minute (LPM) and (*b*) water flowrate = 1.24 LPM

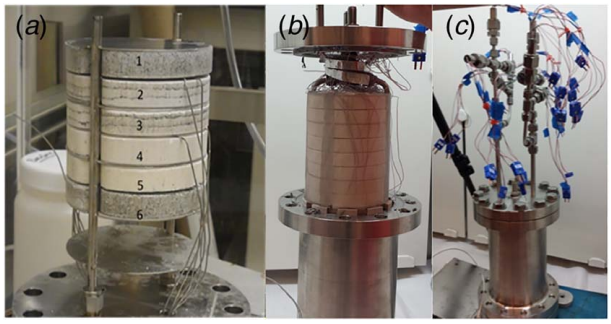

Fig. 7 (*a*) Pucks assembled for conduction enhancement study, from top down (1) bare + randomENG, (2) pin + layerENG, (3) bare + layerENG, (4) bare, (5) bare + pin, and (6) pin + randomENG. (*b*) Assembly into the tank. (c) Testing apparatus with temperature sensors.

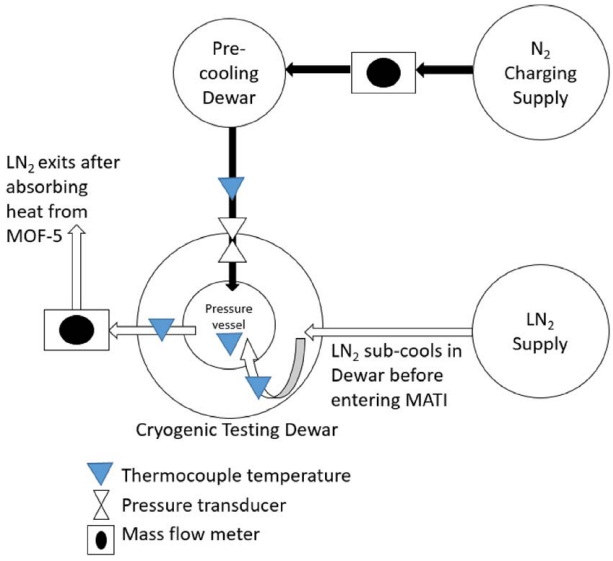

Fig. 8 General flow diagram for MATI testing

pucks and run along the annular region of the tank to the exit port in the flange. It should be noted that accurate placement depth was crucial for the thermocouple placements in order to provide a good comparison between each puck. After the MATI was fully assembled and instrumented, the flange/MATI assembly was carefully removed from the glove box and assembled to the tank.

The MATI conduction enhancement study used the testing facility, which was previously constructed in the schematic flow diagram illustrated in Fig. 8, and the completed system is depicted in Fig. 9. Since liquid nitrogen (LN_2) was selected as the coolant for the hydrogen adsorption process, two vacuum-insulated Dewar vessels were utilized throughout the experiment to house the integrated testing vessel, LN_2 sub-cooling system, and H_2 precooling system. It should be mentioned here that due to tank leakage concerns associated with hydrogen, all adsorption experiments performed below were actually done using nitrogen gas at 25 bars instead of hydrogen gas at the targeted 60 bars. Nevertheless, this preserved the essence of studying the conduction enhancement for MATI design and its potential impact. By placing the secondary cooling systems in close proximity to the 2-L pressure vessel containing the integrated MATI system, it helped maintain a constant 80 K delivery temperature of LN_2 and fully liquid state to the MATI. This also helped maintain cooler temperatures for the absorption gas prior to entering the tank.

The sub-cooling of pressurized LN_2 was achieved using coiled copper tubing submerged in atmospheric LN_2 in the integrated Dewar vessel as shown in Fig. 10(*a*). Providing subcooled LN_2 to

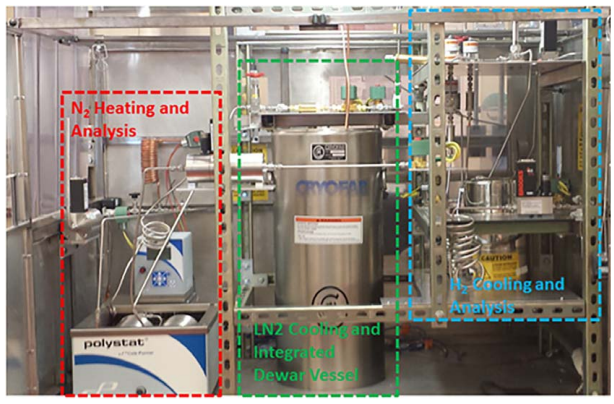

Fig. 9 Constructed MATI testing facility

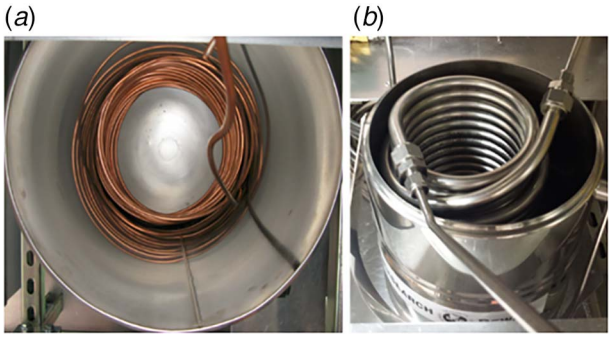

Fig. 10 (*a*) LN2 sub-cooling and (*b*) nitrogen gas precooling coils during MATI conduction enhancement testing

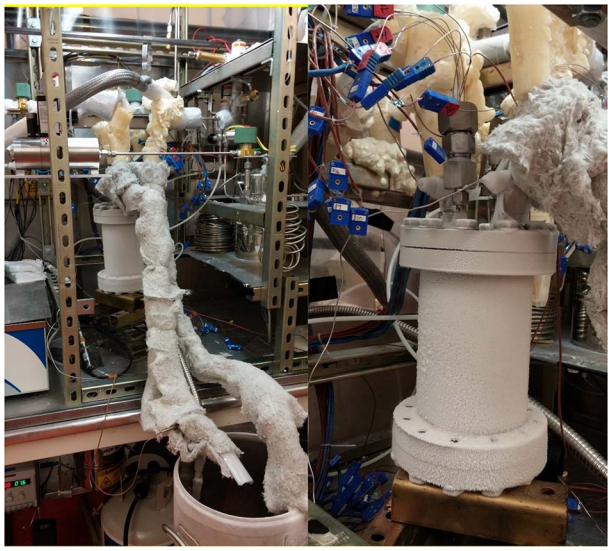

Fig. 11 MATI during open adsorption experiment with sub-cooled LN2 and precooled N2 at 25 bars

the MATI system increases the allowable temperature change of the LN_2 flowing through MATI and minimize the potential for boiling LN_2 in the MATI cooling plate throughout the charging experiments. The adsorbent gas precooling system was accomplished with the flow of gas through submerged tubing coils packed with stainless-steel ball bearings to increase the contact surface area, as shown in Fig. 10(*b*). The used LN_2 was subsequently heated upon exiting the integrated system and passed through a mass flowmeter for flowrate measurement. This was done by using a large capacity heated oil bath to ensure desired nitrogen gas exit temperature. Similarly, a mass flowmeter was utilized to measure the mass flowrate of the adsorbent gas throughout pressurization and charging of the system. The initiation of LN_2 coolant and absorbent nitrogen gas were controlled with electronic solenoid valves via a LabView program.

For the initial test, the integrated MATI testing vessel was not submerged in the LN_2. The pictures illustrating the open experiment are shown in Fig. 11. For demonstration, the vessel was left without thermal insulation. As a result of using LN_2 for cooling, frost was formed outside the vessel. Further testing was conducted with the MATI vessel submerged into atmospheric LN_2 to precool the large thermal mass associated with the stainless-steel tank and thus maintain a constant wall temperature throughout the experiment. During both experiments, LN_2 was subcooled before entering the MATI cooling plates while nitrogen gas was also precooled using atmospheric LN_2 before entering the vessel for adsorption at 25 bars. All experiments were run until the temperatures of the pucks reached a steady-state.

Experimental Uncertainty

A comparison of the temperature response of the different pucks was the focus of this study. Therefore, data corresponding to flowrate and pressure are not presented here, and the focus of the uncertainty analysis is on the temperature measurements.

Bias errors of the instrumentation are thought to be the main cause of error in this study, resulting from the thermocouples, the data acquisition system, and the placement of the thermocouples in the pucks. The T-type thermocouples used have a standard limit of error of ±1 K. The data acquisition module has a max error of ±0.25% of reading for gain error and offset error, each. The maximum temperature reading from the data was 300 K. Summing these errors shows a maximum error of 2.5 K for the bias error.

Another source of measurement uncertainty for MOF bed temperatures is the placement of the thermocouples (as shown in Fig. 7(*a*)). While it is difficult to assess the depth of the thermocouples in the MOF beds during experiment, the thermocouple depths were controlled by a precision tool created to bend the thermocouples in a consistent length. This tool was machined with a tolerance of ±0.005″. Thus, the uncertainty due to thermocouple placement is expected to be minimal.

Results and Discussions

The experimental data presented here includes two different adsorption tests using nitrogen gas. The objective was to compare

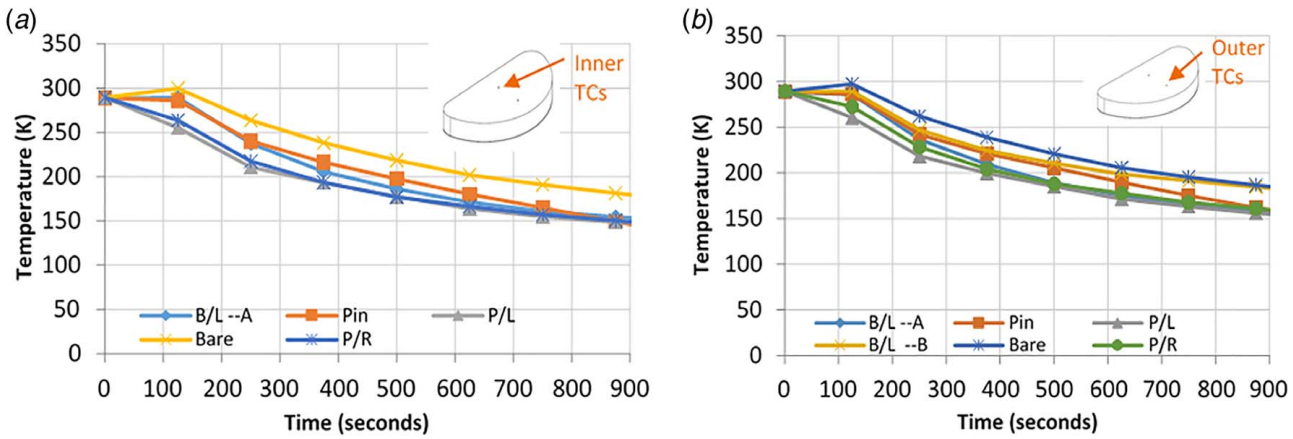

Fig. 12 Puck temperature profiles with MATI vessel open to atmosphere: (*a*) inner thermocouple readings and (*b*) outer thermocouple readings

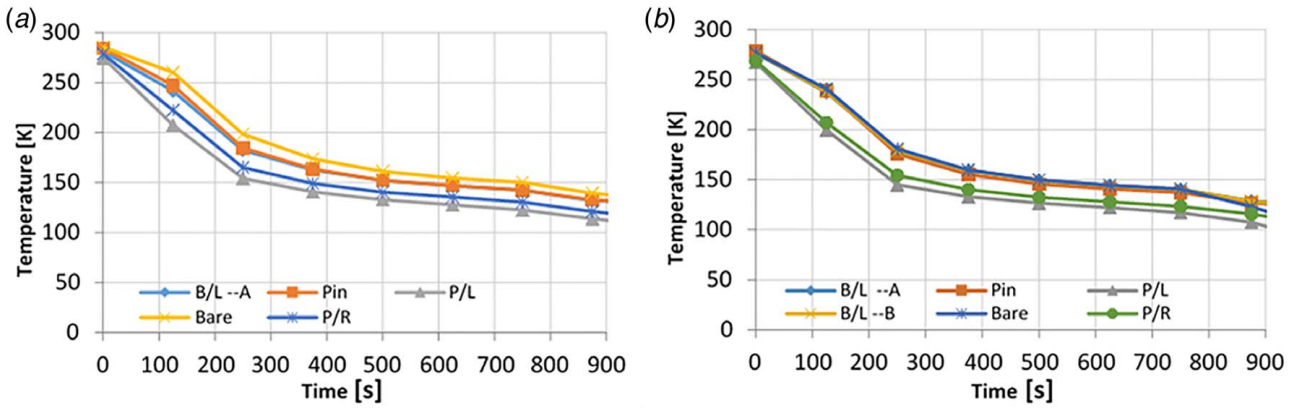

Fig. 13 Puck temperature profiles with MATI vessel submerged in LN2: (*a*) inner thermocouple readings and (*b*) outer thermocouple readings

the thermal performance of each of the six kinds of MOF-5 pucks through conduction enhancement. The measurements of puck temperatures using the embedded thermocouples provided the direct effects of conduction enhancement. As shown, a faster temperature response (decreasing) with LN_2 cooling corresponds to better thermal performance due to conduction enhancement.

The results from the conduction enhancement test without the MATI vessel submerged in LN_2 are presented in Fig. 12. Both the inner and outer thermocouples show that all conduction-enhanced pucks outperformed the bare puck with a faster temperature response to cooling. The puck with pins and layered ENG (P/L) presented superior performance compared to the others. This result is due to its advantage of being able to conduct heat effectively in both vertical and horizontal directions. Pucks with pins and random ENG (P/R) also performed well as expected, which again attributes to the combined approach for conduction enhancement. The pins-only puck, although showing significant thermal improvement over the bare puck, did not seem to provide as much conduction enhancement. However, further examination of the geometries of the pucks and the locations of the two thermocouples showed that one thermocouple is roughly half-way between two pins and the other is one-third of the distance between pins. The two temperature measurements did not seem to adequately capture the 3D nature of the temperature profile within the pins-only pucks. Because of that, it neglected the fact that the regions closer to the pins actually had significantly lower temperatures (indicated also by the simulation results). Essentially from gas adsorption rate standpoint, the pins-only puck is expected to achieve significantly higher gas uptake for a given time.

The results for the test with the vessel submerged into LN_2 are shown in Fig. 13. Similar conduction enhancement trends were observed indicating the data were repeatable. Compared to the previous case where the MATI vessel added significant thermal mass, the submerged test showed no sign of temperature increase from the initial puck temperatures caused by the heat of adsorption. All of the pucks cooled down at a much faster rate as a result of minimizing the additional thermal mass that the LN_2 had to cool.

Conclusions

Metal-organic framework 5, as the leading hydrogen storage material, was studied in the densified form (pucks). While it has a desirable storage capacity of hydrogen, its poor thermal conductivity remains a major challenge in meeting DOE targets. A conduction enhancement study was carried out on the unique MATI design developed through the DOE HSECOE program. Six types of pucks were formed by Ford Company with five of them being conduction enhanced using combinations of aluminum pins and ENG. Significant enhancement was achieved for all five conduction-enhanced pucks using liquid nitrogen as the coolant, confirming the original data predicted by transient thermal simulation of puck sensible cooling using ANSYS. The results could support a near-term hydrogen storage system based on the MATI concept with conduction enhancement that could reach DOE-targeted goals for H_2 fill time, volumetric, and gravimetric storage capacity.

Acknowledgment

The authors would like to thank the DOE Hydrogen Storage Engineering Center of Excellence for its financial support and everyone who contributed to the MATI system development at Oregon State University.

Nomenclature

H_2 = hydrogen
LN_2 = liquid nitrogen

References

[1] Tamburello, D., Hardy, B., Sulic, M., Kesterson, M., Corgnale, C., and Anton, D., 2018, "Compact Cryo-adsorbent Hydrogen Storage Systems for Fuel Cell Vehicles," Paper No. POWER2018-7474, V001T06A025; pp. 1–9, vol. 1.
[2] Tamburello, D., Hardy, B., Corgnale, C., Sulic, M., and Anton, D., 2017, "Cryo-adsorbent Hydrogen Storage Systems for Fuel Cell Vehicles," Paper No. FEDSM2017-69411, V01BT08A005; pp. 1-10. vol. 1B-2017.
[3] Corgnale, C., Hardy, B., Chahine, R., Zacharia, R., and Cossement, D., 2019, "Hydrogen Storage in a Two-Liter Adsorbent Prototype Tank for Fuel Cell Driven Vehicles," Appl. Energy, **250**, pp. 333–343.
[4] Chen, Z., Li, P., Anderson, R., Wang, X., Zhang, X., Robison, L., Redfern, L. R., Moribe, S., Islamoglu, T., Gomez-Gualdron, D. A., Yildirim, T., Stoddart, J. F., and Farha, O. K., 2020, "Balancing Volumetric and Gravimetric Uptake in Highly Porous Materials for Clean Energy," Science, **368**(6488), pp. 297–303.
[5] Ahmed, A., Liu, Y., Purewal, J., Tran, L., Wong-Foy, A., Veenstra, M., Matzger, A., and Siegel, D., 2017, "Balancing Gravimetric and Volumetric Hydrogen Density in MOFs," Energy Environ. Sci., **10**(11), pp. 2459–2471.
[6] Corgnale, C., Hardy, B., Chahine, R., Cossement, D., Tamburello, D., and Anton, D., 2014, "Simulation of Hydrogen Adsorption Systems Adopting the Flow Through Cooling Concept," Int. J. Hydrogen Energy, **39**(30), pp. 17083–17091.
[7] Corgnale, C., Hardy, B., Chahine, R., and Cossement, D., 2018, "Hydrogen Desorption Using Honeycomb Finned Heat Exchangers Integrated in Adsorbent Storage Systems," Appl. Energy, **213**, pp. 426–434.
[8] Li, H., Eddaoudi, M., O'Keeffe, M., and Yaghi, O. M., 1999, "Design and Synthesis of an Exceptionally Stable and Highly Porous Metal-Organic Framework," Nature, **402**(6759), pp. 276–279.
[9] James, S. L., 2003, "Metal-Organic Frameworks," Chem. Soc. Rev., **32**(5), pp. 276–288.
[10] Saha, D., Bao, Z., Jia, F., and Deng, S., 2010, "Adsorption of CO2, CH4, N2O, and N2 on MOF-5, MOF-177, and Zeolite 5A," Environ. Sci. Technol., **44**(5), pp. 1820–1826.
[11] Yang, J., Sudik, A., Wolverton, C., and Siegel, D. J., 2010, "High Capacity Hydrogen Storage Materials: Attributes for Automotive Applications and Techniques for Materials Discovery," Chem. Soc. Rev., **39**(2), pp. 656–675.
[12] Li, J., Cheng, S., Zhao, Q., Long, P., and Dong, J., 2009, "Synthesis and Hydrogen-Storage Behavior of Metal–Organic Framework MOF-5," Int. J. Hydrogen Energy, **34**(3), pp. 1377–1382.

[13] Saha, D., Deng, S., and Yang, Z., 2009, "Hydrogen Adsorption on Metal-Organic Framework (MOF-5) Synthesized by DMF Approach," J. Porous Mater., **16**(2), pp. 141–149.
[14] Sillar, K., Hofmann, A., and Sauer, J., 2009, "Ab initio Study of Hydrogen Adsorption in MOF-5," J. Am. Chem. Soc., **131**(11), pp. 4143–4150.
[15] DeSantis, D., Mason, J. A., James, B. D., Houchins, C., Long, J. R., and Veenstra, M., 2017, "Techno-economic Analysis of Metal-Organic Frameworks for Hydrogen and Natural Gas Storage," Energy and Fuels, **31**(2), pp. 2024–2032.
[16] Ming, Y., Purewal, J., Yang, J., Xu, C., Veenstra, M., Gaab, M., Muller, U., and Siegel, D. J., 2016, "Stability of MOF-5 in a Hydrogen Gas Environment Containing Fueling Station Impurities," Int. J. Hydrogen Energy, **41**(22), pp. 9374–9382.
[17] Sridhar, P., and Kaisare, N. S., 2020, "A Critical Analysis of Transport Models for Refueling of MOF-5 Based Hydrogen Adsorption System," J. Ind. Eng. Chem., **85**, pp. 170–180.
[18] Montes-Andrés, H., Leo, P., Orcajo, G., Rodriguez-Dieguez, A., Choquesillo-Lazarte, D., Martos, C., Botas, J. A., Martinez, F., and Calleja, G., 2019, "Novel and Versatile Cobalt Azobenzene-Based Metal-Organic Framework as Hydrogen Adsorbent," ChemPhysChem, **20**(10), pp. 1334–1339.
[19] Yu, S., Li, S., Meng, X., Wan, C., and Ju, X., 2018, "Tuning the Hydrogen Adsorption Properties of Zn–Based Metal–Organic Frameworks: Combined DFT and GCMC Simulations," J. Solid State Chem., **266**, pp. 31–36.
[20] Chen, S., Shi, Y., and Gu, B., 2018, "Simulation on Hydrogen Storage Properties of Metal-Organic Frameworks Cu-BTC at 77–298K," AIChE J., **64**(4), pp. 1383–1388.
[21] Kaye, S. S., Dailly, A., Yaghi, O. M., and Long, J. R., 2007, "Impact of Preparation and Handling on the Hydrogen Storage Properties of Zn4O(1,4-Benzenedicarboxylate)3 (MOF-5)," J. Am. Chem. Soc., **129**(46), pp. 14176–14177.
[22] Schmitz, B., Müller, U., Trukhan, N., Schubert, M., Férey, G., and Hirscher, M., 2008, "Heat of Adsorption for Hydrogen in Microporous High-Surface-Area Materials," ChemPhysChem, **9**(15), pp. 2181–2184.
[23] "Hydrogen Storage," *Energy.gov*. https://www.energy.gov/eere/fuelcells/hydrogen-storage, Accessed July 11, 2020.
[24] Gómez-Gualdrón, D. A., Wang, T. C., Garcia-Holley, P., Sawelewa, R. M., Argueta, E., Snurr, R. Q., Hupp, J. T., Yildirim, T., and Farha, O. K., 2017, "Understanding Volumetric and Gravimetric Hydrogen Adsorption Trade-Off in Metal-Organic Frameworks," ACS Appl. Mater. Interfaces, **9**(39), pp. 33419–33428.
[25] Palla, S., and Kaisare, N. S., 2020, "Evaluating the Impact of Pellet Densification and Graphite Addition for Design of On-Board Hydrogen Storage in a Fixed Bed of MOF-5 Pellets," Int. J. Hydrogen Energy, **45**, pp. 25875–25889.
[26] Purewal, J. J., Liu, D., Yang, J., Sudik, A., Siegel, D. J., Maurer, S., and Muller, U., 2012, "Increased Volumetric Hydrogen Uptake of MOF-5 by Powder Densification," Int. J. Hydrogen Energy, **37**(3), pp. 2723–2727.
[27] Liu, D., Purewal, J. J., Yang, J., Sudik, A., Maurer, S., Mueller, U., Ni, J., and Siegel, D. J., 2012, "MOF-5 Composites Exhibiting Improved Thermal Conductivity," Int. J. Hydrogen Energy, **37**(7), pp. 6109–6117.
[28] Rodrı´guez Sánchez, A., Klein, H.-P., and Groll, M., 2003, "Expanded Graphite as Heat Transfer Matrix in Metal Hydride Beds," Int. J. Hydrogen Energy, **28**(5), pp. 515–527.
[29] Ichikawa, T., Chen, D. M., Isobe, S., Gomibuchi, E., and Fujii, H., 2004, "Hydrogen Storage Properties on Mechanically Milled Graphite," Mater. Sci. Eng.: B, **108**(1), pp. 138–142.
[30] Burtch, N. C., Jasuja, H., and Walton, K. S., 2014, "Water Stability and Adsorption in Metal–Organic Frameworks," Chem. Rev., **114**(20), pp. 10575–10612.